33RD CONGRESS
OF THE INTERNATIONAL COUNCIL
OF THE AERONAUTICAL SCIENCES
STOCKHOLM, SWEDEN, 4-9 SEPTEMBER, 2022

ICAS 2022 SWEDEN

MORE ELECTRIC AIRCRAFT (MEA) SCALING ASPECTS AND WEIGHT IMPACT

Emil Holmgren[1], Dhruv Haldar[1], Lina Bertling Tjernberg[2] & Andreas Johansson[2,3]

[1]KTH Royal Institute of Technology, Stockholm, Sweden
[2]School of Electrical Engineering and Computer Science, KTH Royal Institute of Technology, Stockholm, Sweden
[3]SAAB, Linköping, Sweden

Abstract

This paper is about investigating the differences in fuel consumption of conventional and equivalent electrical subsystems of passenger aircraft. The goal is to develop a framework that can help evaluate fuel consumption of passenger aircraft, both conventional aircraft and More Electric Aircraft (MEA), for a given size of aircraft and a given stretch of flight.
The work presented in this paper originates from pre-studies within MEA research performed by the Reliability Centered Asset Management (RCAM) research group at KTH in collaboration with SAAB that has been done on a passenger aircraft with comparable size to the Airbus A320. The main difference to the prior study is the addition of subsystem weight, passenger scaling effects, environmental dependencies and flight profile, all added to increase the accuracy and diversity of the model. The fuel consumption is based on studies of existing technology for several passenger aircraft from Airbus and Boeing. The main focus was the Environmental Control System (ECS).
A numerical model of passenger aircraft including the ECS was constructed in MATLAB with different levels of electrification, a conventional ECS or a fully electric ECS. A special case with an Airbus A320 with 180 passengers doing a round trip between Copenhagen and Stockholm on a hot day was studied.
The results show possible fuel savings in the magnitude of 4% to 8% when electrifying the ECS for the case studied and for aircraft with 156 to 700 passengers.

Keywords: More Electric Aircraft (MEA), Environmental Control System (ECS), Fuel Consumption Simulation, Subsystem Weight Impact, Passenger Scaling

1. Introduction

The Advisory Council for Aeronautics Research in Europe (ACARE) [1] has set several goals to be accomplished by 2050 for aviation. Some goals proposed are a 75% reduction in carbon dioxide (CO_2) emissions per passenger kilometre, a 90% reduction in nitrogen oxide (NO_x) emissions and a reduction of perceived noise emittance of aircraft by 65%. These goals are relative to typical new passenger aircraft in 2000.
More Electric Aircraft (MEA) technologies aim in reducing greenhouse gas emissions to make air transport more energy-efficient, while still being cost-effective and reliable.
To help decide if it is worth investing in a new subsystem, a framework has been developed to calculate the fuel consumption of conventional and electrical subsystems for a given flight and for the most common passenger aircraft sizes. The framework originates specifically from prior project [2].
Due to time constraints, only the Environmental Control System (ECS), the largest secondary power consumer, has been modelled in detail. Other subsystems are included in the model, but are not described in the same level and are not presented in this paper.

2. Methodology and Problem Formulation

The general questions, leading to this paper, are:

- Can the MEA technology assist the air transportation industry in the reduction of fuel consumption and achieving the climate goals?
- What is the fuel consumption of a passenger aircraft with different levels of electrification?
- Is the weight penalty going to eliminate the positive effect of higher efficiency for new subsystems?
- How does passenger-scaling (pax-scaling) affect the overall fuel consumption of the aircraft?

The fuel consumption is reflected by the power usage of the aircraft and all its subsystems, therefore it is important to understand how they work and what is affecting their power consumption. Power to generate thrust is the largest consumer and is called primary power. Secondary power is all other power that is not used to generate thrust.
Subsystems may differ in technology, efficiency, power management, weight and drag. Since every subsystem on an aircraft are connected and affecting each other in many ways, it is not clear if one system solution is better than the other.
The pax-scaling, which is the factor that more than any other factors determines the aircraft size, is thought to influence the overall efficiency of the aircraft.
Flight conditions, such as ambient temperature, speed and altitude should have an impact on fuel consumption.
To understand how all these factors affect the fuel consumption, detailed energy-models for every subsystem must be developed. When all the subsystems are modelled along with the flight dynamics, a simulation for the complete aircraft can be made for a given flight profile, to obtain the total fuel spent on a flight.
By combining different subsystem technologies and various levels of electrification, multiple virtual aircraft can be simulated side by side and compared.

3. Thrust Fuel Consumption

Thrust fuel consumption can be calculated with:

$$\dot{m}_{fuel,T} = T \cdot TSFC \quad [\mathrm{kg/s}] \tag{1}$$

, where T [N] is the thrust and $TSFC$ [kg/(N·s)] is the Thrust Specific Fuel Consumption of the aircraft jet engine.

According to [3], the $TSFC$ of modern passenger aircraft jet's engines in cruise is around 16 [mg/(N·s)], based on JET-A1 as fuel. Very advanced engines can have a value as low as 14 [mg/(N·s)]. An estimation of $TSFC$ as function of speed and temperature can be shown to be:

$$TSFC = (1.13 \cdot 10^{-5} + 1.25 \cdot 10^{-5} \cdot M) \cdot \sqrt{\frac{T_{amb}}{T_0}} \quad [\mathrm{kg/(N \cdot s)}]$$

, where M is the flight Mach number. T_{amb} $[K]$ is the ambient temperature at altitude and $T_0 = 288$ K.

To determine thrust, a simplified 2D model containing forces acting on the aircraft in flight was established according to fig. 1.

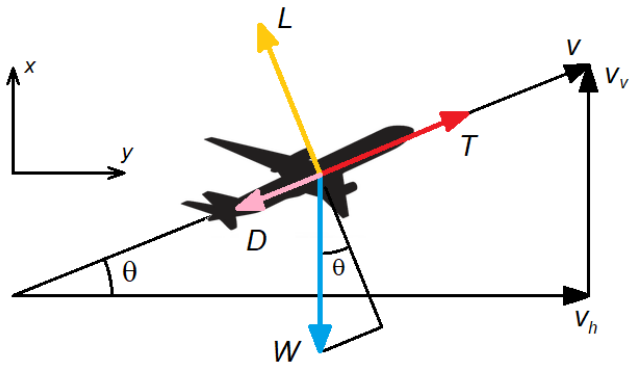

Figure 1 – 2D forces on the aircraft in flight.

Thrust can then be expressed as:

$$T = D + m \cdot (g + a_v) \cdot \sin(\theta) + m \cdot a \quad [\mathrm{N}] \tag{2}$$

, where

D	[N]	is the aircraft drag
m	[kg]	is the aircraft mass
g	[m/s^2]	is the gravitational constant
a_v	[m/s^2]	is the vertical acceleration of the aircraft
θ		is the climb angle of the aircraft
a	[m/s^2]	is the acceleration in the flight direction of the aircraft.

Aircraft drag is a sum of zero-lift drag and lift induced drag. The zero-lift drag is relatively complicated to calculate as it depends on many factors such as aircraft size, configuration and flight profile.

3.1 Weight Impact of Subsystems on the Fuel Consumption

The weight of subsystems contributes to fuel consumption through the required thrust to carry them. Using eq. 1 and 2 in combination with subsystem mass, m_{ss}, and lift induced drag coefficient, C_{Di}, gives the subsystem weight fuel consumption:

$$\dot{m}_{fuel,ss} = TSFC \cdot m_{ss} \cdot ((g + a_v) \cdot (C_{Di} \cdot cos(\theta) + sin(\theta)) + a) \quad [\mathrm{kg/s}]$$

4. Secondary Power Fuel Consumption

There are many kinds of secondary power, and they can be divided into a few categories, depending on how they are transferred to the consumer. The difference between each category is simply their transfer efficiency. Since all secondary power is generated by the jet engine, they can be traced back to the engine shaft power. A flowchart showing the relation between secondary power and fuel consumption can be seen in fig. 2.
Pneumatic power or bleed-air power is proportional to the bleed-air mass flow rate and the bleed-air temperature, while the bleed-air temperature is dependent on the engine and the thrust setting. It is therefore necessary to estimate the thrust setting of the engines and combine it with engine data to obtain the bleed-air temperature.

According to [3], the engine shaft power fuel consumption can be calculated with:

$$\dot{m}_{fuel,shaft} = P_{shaft} \cdot k_p \cdot TSFC \quad [\mathrm{kg/s}] \tag{3}$$

, where P_{shaft} [W] is the engine shaft power and k_p [N/W] is the Shaft Power Factor.

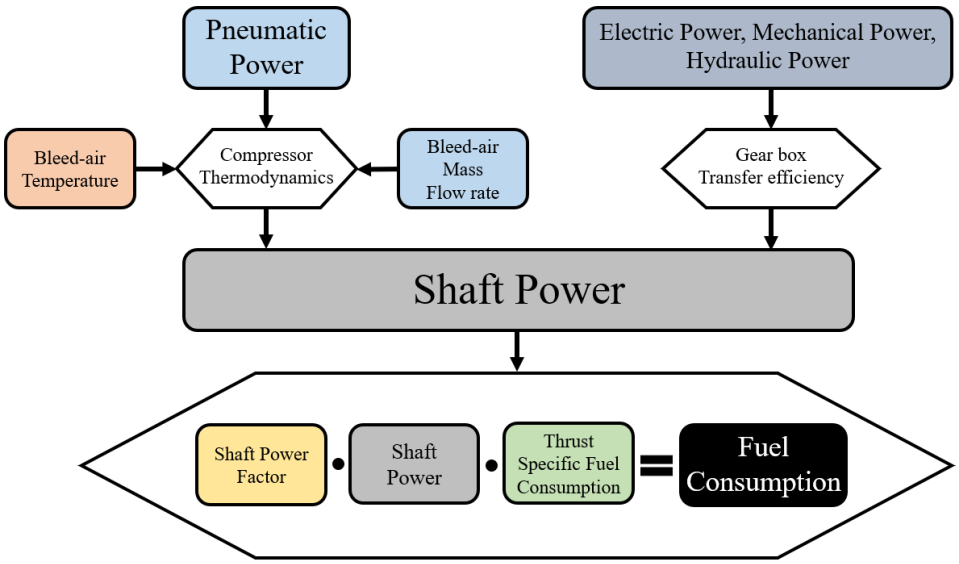

Figure 2 – Flowchart showing how secondary power are related to fuel consumption.

An approximation of the Shaft Power Factor, k_P [N/W], for similar turbofan engines as function of Mach number, M, and altitude, h [m], was derived to be:

$$k_P = 0.0057 + 4.60 \cdot 10^{-8} h - 0.0106M - 4.44 \cdot 10^{-13} h^2 + 1.85 \cdot 10^{-7} hM + 0.0049M^2$$

5. Environmental Control System (ECS) Fuel Consumption

The Environmental Control System (ECS) is responsible for maintaining a pleasant temperature, healthy pressure and good air quality in the cabin. The ECS is designed and operated to meet the requirements specified by the Code of Federal Regulations by the Federal Aviation Administration (FAA) [4].

The operation of the ECS is simulated with a simplified thermodynamic model of the cabin, where the control volume is a function of aircraft size and the heat flux are functions of the flight profile and the number of passengers (pax). The number of passengers decides over the size of the aircraft. The fresh air mass flow rate that is injected into the cabin is determined by the temperature of the injected air and the heat flux balance of the cabin, while the fresh air mass flow rate must be at least 0.55 pounds per minute (4.16 g/s) for each occupant. In this study, the minimum fresh air mass flow rate is chosen to be 6 g/(pax·s) [5].

Three ECS variants are included in this study:

1. Conventional bleed-air driven Air Cycle Machine (ACM)
2. Electrical Air Cycle Machine (E-ACM)
3. Electrical Vapour Cycle Machine (E-VCM)

5.1 Conventional Air Cycle Machine (ACM)

The conventional Air Cycle Machine (ACM) is driven by pressurized air from the engine compressor, also called bleed-air. The ACM is responsible for cooling of the hot bleed-air before it is sent to the cabin. A relatively small amount of electric power is used to control the ECS and to drive electric circulation fans.

To maintain a cabin temperature of 295.15 K (22 °C) under various conditions, the ECS will initially adjust the temperature of the injected fresh air. If adjusting the fresh air temperature is not enough, then the airflow rate can be increased. Air pressure in the cabin is maintained and regulated through

Out-Flow Valves, OFV, located at the bottom rear of the fuselage.

Thermal equilibrium for a hot day and the aircraft stationary on the ground can be described with:

$$\dot{Q}_{ECS} + \dot{Q}_{shadow} + \dot{Q}_{sun} + \dot{Q}_{pax} = 0 \tag{4}$$

, where

$\dot{Q}_{ECS}$	is the heat flux from the ECS
$\dot{Q}_{shadow}$	is the heat flux through the fuselage in the shadow
$\dot{Q}_{sun}$	is the heat flux through the fuselage in the sun
$\dot{Q}_{pax}$	is the passenger associated heat flux.

Heat flux from the ECS can be defined as:

$$\dot{Q}_{ECS} = \dot{m}_{air} \cdot C_p \cdot (T_{ECS} - T_{cabin}) \tag{5}$$

, where $\dot{m}_{air}$ is the air mass flow rate, C_p is specific heat capacity of air, T_{ECS} is air temperature provided by the ECS and T_{cabin} is the cabin temperature.

Heat flux through the part of the fuselage, that is in the shadow, from ambient air is:

$$\dot{Q}_{shadow} = U \cdot (A_{wet} - A_{proj}) \cdot (T_{amb} - T_{cabin}) \tag{6}$$

, where U is the thermal conductivity of the fuselage skin, A_{wet} is the wet surface area of the fuselage, A_{proj} is the projected area of the fuselage, T_{amb} is the ambient temperature and T_{cabin} is the cabin temperature.

Heat flux through the part of the fuselage, that is in the sun, can be expressed as:

$$\dot{Q}_{sun} = U \cdot A_{proj} \cdot (T_{amb} + \Delta T_{solar} - T_{cabin}) \tag{7}$$

, where ΔT_{solar} is the average temperature rise of the surface, due to solar radiation. The temperature rise is approximately 10 K, for a white surface [6].

The passenger associated heat flux, $\dot{Q}_{pax}$, is based on metabolic heat and all other facilities such as entertainment, lighting, galley etc. It is roughly 190 W/pax [7].

5.1.1 ACM Fresh Air Mass Flow Rate

By combining eq. 4-7 and solving for the air mass flow rate, for on ground conditions, gives:

$$\dot{m}_{air,static} = \frac{U \cdot (A_{wet} - A_{proj}) \cdot (T_{amb} - T_{cabin}) + U \cdot A_{proj} \cdot (T_{amb} + \Delta T_{solar} - T_{cabin}) + \dot{Q}_{pax}}{C_p \cdot (T_{cabin} - T_{inlet})} \tag{8}$$

, where cooling is assumed with $T_{inlet} = 259.37$ K (-13.8 °C) [9], for a hot day. T_{inlet} is the temperature of the air that is entering the mixing chamber before it is sent to the cabin.

When flying, it is assumed that forced convection will remove most of the solar heating. The temperature rise due to solar heating will then be relatively small and can be neglected. The ambient temperature, T_{amb}, is replaced with total temperature, T_{tot}, to include the kinetic heating effect, thus the air mass flow rate can be calculated as:

$$\dot{m}_{air,fly} = \frac{U \cdot A_{wet} \cdot (T_{tot} - T_{cabin}) + \dot{Q}_{pax}}{C_p \cdot (T_{cabin} - T_{inlet})} \tag{9}$$

If heating is required (if eq. 8 or 9 gives negative values), then heating with $T_{inlet} = 393.15$ K (120 °C) is assumed [9].

It must be ensured that the fresh air mass flow rate meets the regulation. If the calculated air mass flow rate is smaller than the minimum value, $\dot{m}_{air,min} = 0.006 \cdot pax$ kg/s, then $\dot{m}_{air}$ is set to $\dot{m}_{air,min}$.
With the regulated air mass flow rate, a new inlet temperature is calculated:

$$T_{inlet} = T_{cabin} - \frac{U \cdot A_{wet} \cdot (T_{tot} - T_{cabin}) + \dot{Q}_{pax}}{C_p \cdot \dot{m}_{air,min}}$$

5.1.2 ACM Pre-Cooler and Heat Exchangers

Excessive heat from the bleed-air is expelled through the pre-cooler and the heat exchangers in the ACM. Cooling-air that is flowing through the pre-cooler comes from the engine fan and is costing engine shaft power. Cooling-air through the heat exchangers is taken via air scoops from outside air and is inducing drag to the aircraft.

The air mass flow rate through the pre-cooler and heat exchangers are calculated with the simple assumption that the difference of temperature between the hot air inlet and the cold air outlet is ΔT_{hx}. Further, an adiabatic process is assumed where no heat is transferred to the environment, except in the heat exchanger itself.

For safety reasons, the bleed-air is cooled down in the pre-cooler below the autoignition temperature ($T_{safe} = 200\ ^\circ$C) of jet fuel before it leaves the engine. If cooling of bleed-air is needed ($T_{bleed} > T_{safe}$), then the ratio of engine fan air to bleed-air mass flow rate can be expressed as:

$$\xi_{fan} = \frac{\dot{m}_{fan}}{\dot{m}_{air}} = \frac{T_{bleed} - T_{safe}}{(T_{bleed} - \Delta T_{hx}) - T_{fan}}$$

, otherwise $\xi_{fan} = 0$.

The cooling-air flow rate through the heat exchangers in the ACM is expressed as:

$$\dot{m}_{hx} = \dot{m}_{air} \cdot \frac{T_{safe} - T_{shx}}{(T_{safe} - \Delta T_{hx}) - T_{tot}} \tag{10}$$

, where T_{shx} is the air temperature after the secondary heat exchanger.

5.1.3 ACM Air Scoops Drag

Intake of cooling-air through the air scoops for the heat exchangers induces drag to the aircraft and can be expressed as:

$$D_{scoops} = \dot{m}_{hx} \cdot v \tag{11}$$

, where $\dot{m}_{hx}$ comes from eq. 10, while v is the true air speed of the aircraft.
The fuel consumption that is induced by air scoops drag is calculated according to eq. 1 by:

$$\dot{m}_{fuel,scoops} = D_{scoops} \cdot TSFC \quad [\mathrm{kg/s}] \tag{12}$$

5.1.4 ACM Shaft Power

For bleed-air, shaft power is a function of air mass flow rate and bleed temperature. According to [7], exergy (in this case, engine shaft power) can be calculated using:

$$Exergy = P_{shaft} = \dot{m}_{air} \cdot [(h - h_0) + T_0 \cdot (s - s_0)] \tag{13}$$

, where

P_{shaft} is the shaft power
$\dot{m}_{air}$ is the bleed-air mass flow rate
h is the enthalpy of bleed-air
h_0 is the enthalpy of air at compressor inlet
T_0 is the temperature at compressor inlet
s is the entropy of bleed-air
s_0 is the entropy of air at compressor inlet

Enthalpy and entropy can be obtained from data tables when all the temperatures are known. The compressor inlet temperature is the total temperature (static + kinetic), while the compressor outlet temperature is the same as bleed temperature.

When an Auxiliary Power Unit (APU) is providing bleed-air, the bleed-air temperature is:

$$T_{bleed} = 1.352 \cdot T_{tot}$$

, assuming that the pressure ratio is 2.5 [8], and the compressor efficiency is 0.85. When the engines are running, the bleed temperature will be set by the engines and various conditions.

The shaft power for the conventional ACM ECS is a sum of 3 different terms, shaft power for fresh air (bleed-air), shaft power for pre-cooler (bleed-air from engine fan) and shaft power for electric circulation fans:

$$P_{shaft,ACM} = P_{shaft,bleed} + P_{shaft,fan} + P_{shaft,cf}$$

With help from eq. 13 these terms can be expressed as:

$$P_{shaft,bleed} = \dot{m}_{air} \cdot [(h_{bleed} - h_{tot}) + T_{tot} \cdot (s_{bleed} - s_{tot})]$$

$$P_{shaft,fan} = \xi_{fan} \cdot \dot{m}_{air} \cdot [(h_{fan} - h_{tot}) + T_{tot} \cdot (s_{fan} - s_{tot})]$$

, where

h_{bleed} is the enthalpy of bleed-air
h_{fan} is the enthalpy of the engine fan-air
h_{tot} is the enthalpy of air at the compressor inlet
T_{tot} is the temperature at the compressor inlet
s_{bleed} is the entropy of bleed-air
s_{fan} is the entropy of the engine fan-air
s_{tot} is the entropy of air at the compressor inlet

The engine shaft power to run the circulation fans is:

$$P_{shaft,cf} = \frac{P_{cf}}{\eta_{gbx} \cdot \eta_{gen} \cdot \eta_{trn} \cdot \eta_{mot}} \tag{14}$$

, where

P_{cf} is the power of the circulation fans
η_{gbx} is the accessory gearbox efficiency
η_{gen} is the generator efficiency
η_{trn} is the electric power transfer efficiency
η_{mot} is the motor efficiency

When the engine shaft power for the ACM ECS is known, then the fuel consumption is calculated with eq. 3.

5.2 Electrical Air Cycle Machine (E-ACM)

The electric ACM works in the same way as the conventional version. The compressed air mass flow rate is the same as for the ACM. The only difference is the source of the compressed air and the shaft power calculation, since the power is taking a different path from the engine.

Beginning with the supply of compressed fresh air from the electrical compressor. The supply pressure is about 150 kPa above cabin pressure [8]. The pressure ratio for the supply air is then:

$$\pi_{comp} = \frac{P_{cabin} + 150 \text{ kPa}}{P_{tot}}$$

Depending on flight condition and compressor efficiency, the compressed air temperature can be expressed as:

$$T_{comp} = T_{tot} \cdot \left[1 + \frac{\pi_{comp}^{\frac{\gamma-1}{\gamma}} - 1}{\eta_{comp}} \right] \tag{15}$$

, where π_{comp} is the pressure ratio, $\gamma = \frac{C_p}{C_v}$ is the ratio of specific heat for air. It changes with temperature, but can be approximated to $\gamma \approx 1.4$ in this case. η_{comp} is the compressor efficiency.

5.2.1 E-ACM Heat Exchangers

With the same procedure as with the conventional ACM, the cooling-air mass flow rate through the heat exchangers is calculated as:

$$\dot{m}_{hx} = \dot{m}_{air} \cdot \frac{T_{comp} - T_{shx}}{(T_{comp} - \Delta T_{hx}) - T_{tot}}$$

, where T_{comp} comes from eq. 15.

5.2.2 E-ACM Air Scoops Drag

The amount of air mass flow rate through air scoops for the E-ACM is the sum of cooling-air, $\dot{m}_{hx}$, and fresh air, $\dot{m}_{air}$. This leads to a drag calculation, similar to eq. 11:

$$D_{scoops} = v \cdot (\dot{m}_{hx} + \dot{m}_{air})$$

The fuel consumption that is induced by air scoops drag is calculated with eq. 12.

5.2.3 E-ACM Shaft Power

With eq. 13, the compressor power can be calculated as:

$$P_{comp} = \dot{m}_{air} \cdot [(h_{comp} - h_{tot}) + T_{tot} \cdot (s_{comp} - s_{tot})]$$

This power comes from the engine shaft, through a gearbox, a generator, cables, power converters and a motor, all having an efficiency less than unity. Finally, shaft power that is extracted from the engine to the compressor and for the E-ACM can be calculated using:

$$P_{shaft,comp} = \frac{P_{comp}}{\eta_{gbx} \cdot \eta_{gen} \cdot \eta_{trn} \cdot \eta_{mot}}$$

$$P_{shaft,EACM} = P_{shaft,comp} + P_{shaft,cf}$$

, where shaft power for the circulation fans, $P_{shaft,cf}$, is the same as in eq. 14.

The same way as with the conventional ECS, the fuel consumption of the electric version is calculated with eq. 3.

5.3 Electrical Vapour Cycle Machine (E-VCM)

Like the E-ACM, the E-VCM also uses an electric air compressor to deliver air to the cabin, but at a lower pressure, since the pressurized air is not used to drive the machine, as for the E-ACM. Cooling is done through the Vapour Cycle Machine (VCM). The fresh air mass flow rate and inlet temperature are the same for the VCM as for the previous machines, since they are all simulated with the same cabin model.

5.3.1 E-VCM Operation

The supply pressure is about 20 kPa above the cabin pressure [8]. The pressure ratio for the supply air is then:

$$\pi_{comp} = \frac{P_{cabin} + 20 \text{ kPa}}{P_{tot}}$$

The compressed air temperature, T_{comp}, is calculated as in eq. 15.

If cooling is needed by the VCM, then the cooling power is expressed as:

$$\dot{Q}_{VCM} = \dot{m}_{air} \cdot C_p \cdot ((T_{tot} + \Delta T_{hx}) - T_{inlet})$$

The power to run the vapour cycle compressor is calculated as:

$$P_{comp,VCM} = \frac{\dot{Q}_{VCM}}{\text{COP}_\text{R}}$$

Coefficient of Performance Refrigerator (COP_R) can vary depending on temperatures and refrigerant, but be set to 3, for simplicity. This means that 1 kW of power input to the VCM motor can pull out 3 kW of heat from the supplied air.

Since the compressed air temperature is not as high as for the previous cycle machines, cooling through heat exchangers is not always necessary. Often, heat exchangers must be throttled or even turned off. The cooling-air mass flow rate through the primary heat exchanger is:

$$\dot{m}_{phx} = \dot{m}_{air} \cdot \frac{T_{comp} - (T_{tot} + \Delta T_{hx})}{(T_{comp} - \Delta T_{hx}) - T_{tot}} = \dot{m}_{air}$$

While the cooling-air mass flow rate through the secondary heat exchanger is:

$$\dot{m}_{shx} = \frac{\dot{Q}_{VCM} \cdot (1 + 1/COP_r)}{C_p \cdot (T_{shx} - T_{tot})}$$

If no cooling is required, then the vapour cycle compressor is turned off, $P_{comp,VCM} = 0$ and as a consequence, there is no cooling-air flow through the secondary heat exchanger, $\dot{m}_{shx} = 0$.
Cooling-air mass flow rate through the primary heat exchanger is throttled according to:

$$\dot{m}_{phx} = \dot{m}_{air} \cdot \frac{T_{comp} - T_{inlet}}{(T_{comp} - \Delta T_{hx}) - T_{tot}}$$

In freezing conditions, such as cruising at high altitudes, an electric heater is most likely needed to add more heat to the cabin. If heating is needed, then the primary heat exchanger is bypassed, $\dot{m}_{phx} = 0$, and the electric heater is turned on with a power of:

$$P_{eh} = -U \cdot A_{wet} \cdot (T_{tot} - T_{cabin}) - \dot{m}_{air} \cdot C_p \cdot (T_{comp} - T_{cabin}) - \dot{Q}_{pax}$$

5.3.2 E-VCM Air Scoops Drag

The amount of air mass flow rate through air scoops for the E-VCM is the sum of cooling-air through the primary heat exchanger and secondary heat exchanger plus fresh air. The drag calculation is similar to eq. 11:

$$D_{scoops} = v \cdot (\dot{m}_{phx} + \dot{m}_{shx} + \dot{m}_{air})$$

The fuel consumption that is induced by air scoops drag is calculated with eq. 12.

5.3.3 E-VCM Shaft Power

Power to compress supply air is expressed as:

$$P_{comp} = \dot{m}_{air} \cdot [(h_{comp} - h_{tot}) + T_{tot} \cdot (s_{comp} - s_{tot})]$$

The total shaft power to run the E-VCM is:

$$P_{shaft,EVCM} = \frac{P_{comp} + P_{comp,VCM} + P_{cf} + P_{hxf}}{\eta_{gbx} \cdot \eta_{gen} \cdot \eta_{trn} \cdot \eta_{mot}} + \frac{P_{eh}}{\eta_{gbx} \cdot \eta_{gen} \cdot \eta_{trn}}$$

, where power for the circulation fans ,P_{cf}, is the same as for the conventional ACM. Power to pull cooling-air through the heat exchangers is P_{hxf}.

When the total shaft power to run the E-VCM is known, then the fuel consumption of the E-VCM ECS is calculated with eq. 3.

6. Numerical Model

Everything on and around an aircraft is connected and interacts with each other in a variety of complexity. To make the result more interesting, all the details must be at a certain level, which will require the calculations to be automated.

The complicated nature of the problem is tackled by dividing it up into several modules, each one focusing on a specific task. The modular structure also facilitates the reusing of code and improves its readability. See fig. 3. The flow of information between the modules is visualized by the arrows in the figure.

The Numerical Model will form the Framework to compare various aircraft setups under different flight conditions. Several aircraft can be executed in parallel, making comparison easy.

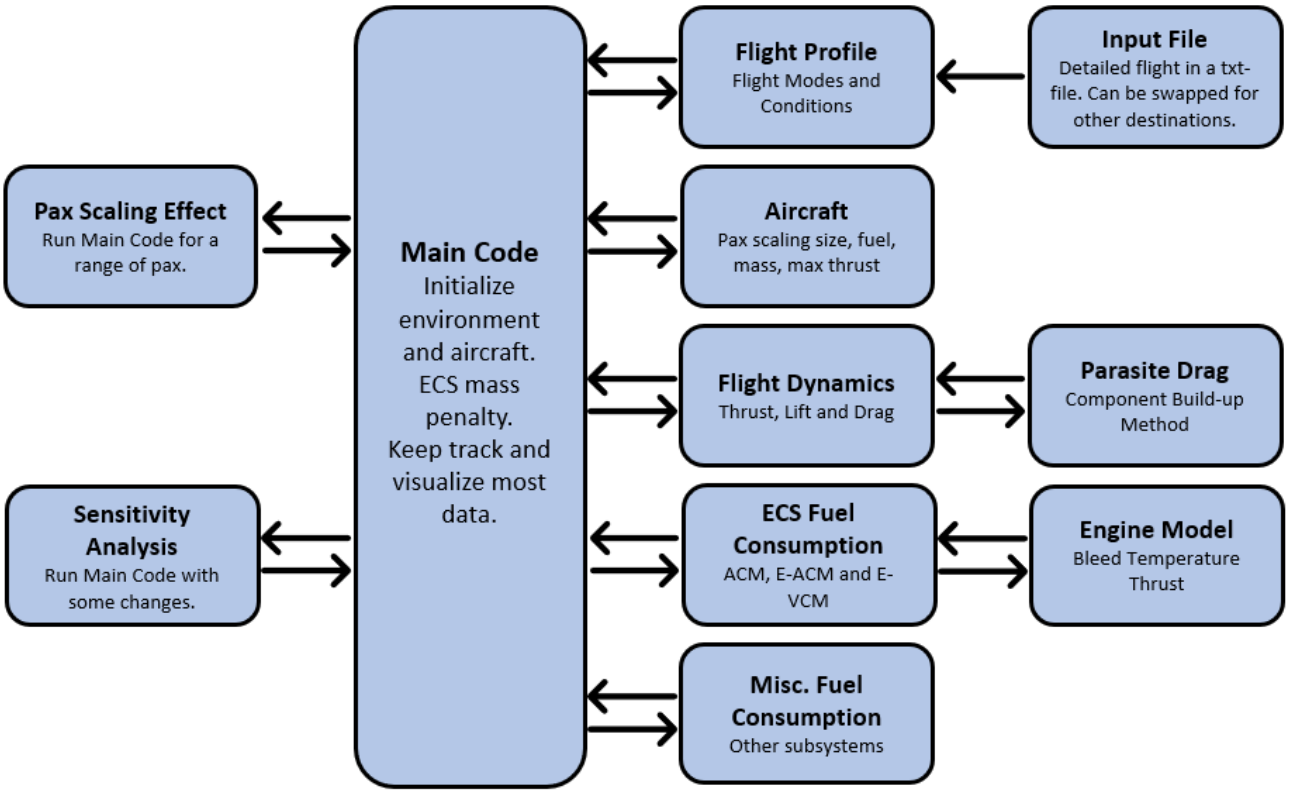

Figure 3 – The MATLAB code is built with several modules to break down the problem into uncomplicated steps.

7. Simulation Result

A case study was done with the Airbus A320 and 180 passengers (pax) on a round trip Copenhagen-Stockholm-Copenhagen. Three different passenger aircraft were simulated in parallel. They are all based on the same aircraft, but with different ECS, flying on the same path. A hot day (30 °C on the ground) was chosen because it was thought that the heat will stress the ECS to work harder, magnifying the systems' differences.

7.1 ECS Fuel Consumption

Fig. 4 shows a breakdown of the fuel consumption of all 3 ECS configurations. The labels in the figure are explained by:

Operation is the fuel required to operate the ECS.

Weight Penalty is the fuel spent to carry the weight of the ECS.

Air Scoops Drag is the fuel consumption induced by the intake of the outside air through air scoops.

ECS Forced Thrust is the increased thrust fuel consumption, forced by the ECS.

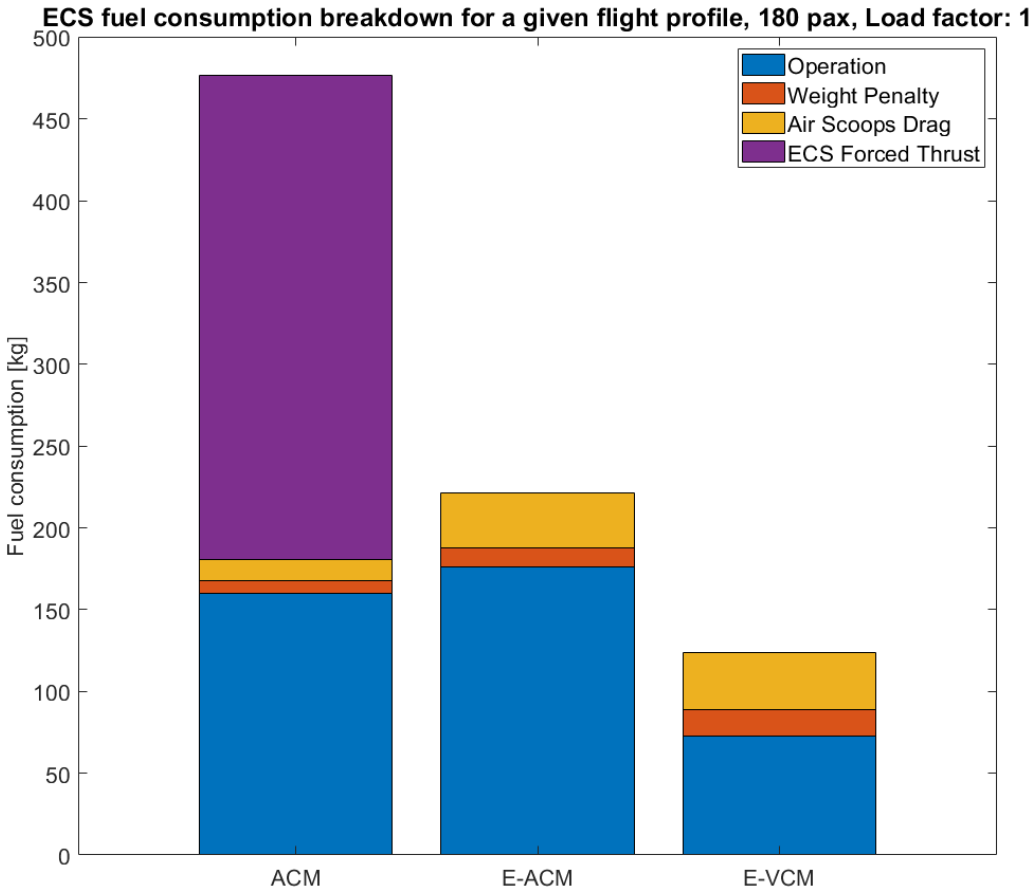

Figure 4 – ECS fuel consumption breakdown for a round trip flight, Copenhagen-Stockholm-Copenhagen, with a modelled A320 and 180 pax.

The ACM is more efficient than the E-ACM. If the effect of weight and drag are added, then the E-ACM becomes even more inferior. However, in this particular case, for the bleed-air driven ACM, there were some moments when the ECS forced the engines to run at a higher thrust setting than was required by the aircraft. If this thrust increased fuel consumption is taken into consideration, then the conventional ACM has a clear disadvantage over the electrical options.

The VCM has the most efficient operation, consuming about half the fuel amount of the ACM. But the increased weight penalty and drag offset some operational efficiency.

7.2 ECS Partial Results

This section will show and discuss significant partial results from a simulation of the case study.

7.2.1 Air Mass Flow Rates

Beginning with the Air Mass Flow Rates for the case study. Fig. 5 shows the air mass flow rates for all 3 systems. When the ECS is active, the minimum fresh air flow rate for the cabin is $\dot{m}_{air,min} = 0.006 \cdot 180 = 1.08$ kg/s, otherwise it is zero. During the cruise, when heating is required, all systems will run at $\dot{m}_{air,min}$. When cooling is needed at lower altitudes, the flow rates are higher. All three systems use the same amount of fresh air. Ram air for the ACM heat exchanger and ram air for the VCM heat exchangers are also shown. The hot side of the VCM is not allowed to be more than 80 °C, which is a relatively low temperature; this explains why the secondary heat exchanger requires much cooling-air.

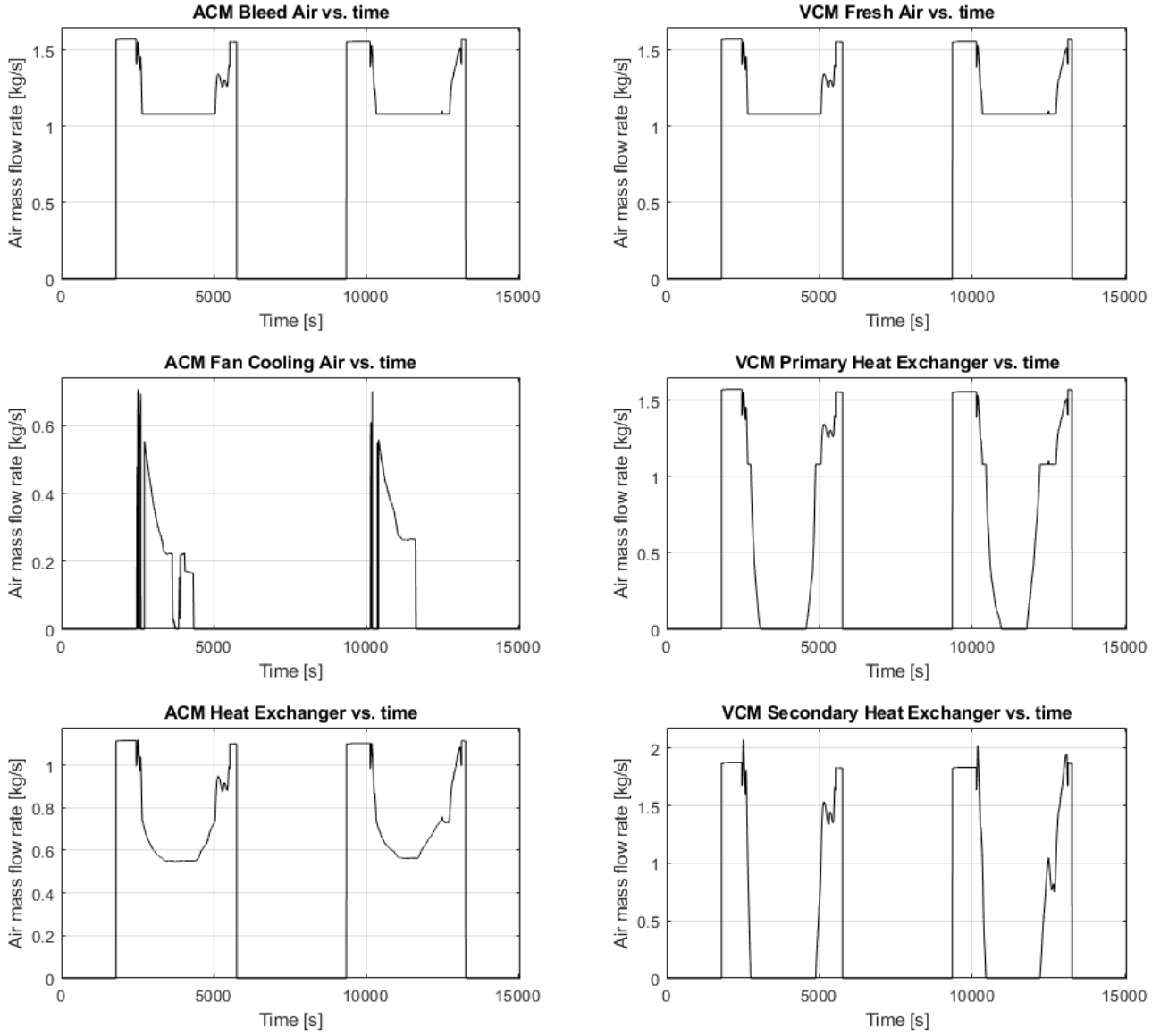

Figure 5 – ECS air mass flow rates for the case study. The load factor is 100%.

7.2.2 Compressed Air Temperatures

The numerical model for the engine is based on engine maps for the CFM International CFM56-5B engine. Compressed air temperature from various parts can be seen in fig. 6. Each flight begins with the APU starting up and providing compressed air for the aircraft. Right before taxiing, the engines start and take over the role to provide power for the aircraft. Small steps can be seen in the graph. During takeoff, the engines are suddenly working much harder, which also increases the bleed-air temperature. It can be seen as spikes in the graph. A few seconds later, when the Low Pressure Compressor (LPC) pressure is high enough, switching over from High Pressure Compressor (HPC) to LPC occurs. This explains the sudden drop in the bleed-air temperature. Switching back to HPC from LPC instantly increases the bleed-air temperature.

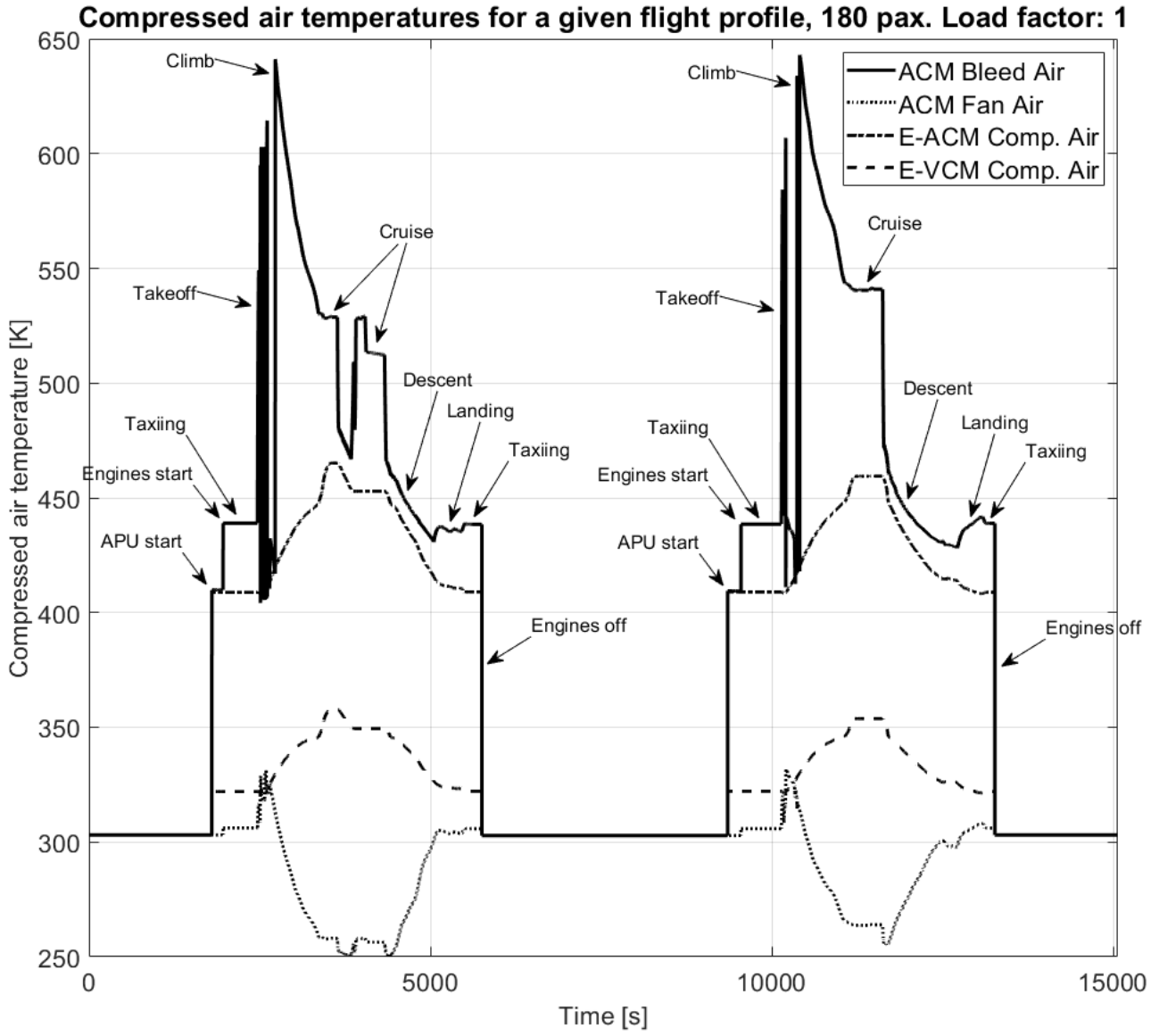

Figure 6 – Compressed air temperatures for the case study.

7.2.3 Bleed Ports Air Pressure

Pressure for the CFM56-5B engine bleed ports can be seen in fig. 7. It is desirable to extract bleed-air at the LPC, since lower bleed-pressure means lower bleed-temperature and lower fuel consumption. But, the bleed-pressure must exceed the lower limit, to be able to drive the ACM. It is set to 250 kPa [8].

The bleed pressure is relatively constant during cruise, except for when the aircraft changes flight level. During the descent, the engines are idling or have just enough power to keep the bleed pressure limit. For landing, thrust and pressure increase slightly and continues during the taxi until the aircraft turns off the engines at the gate.

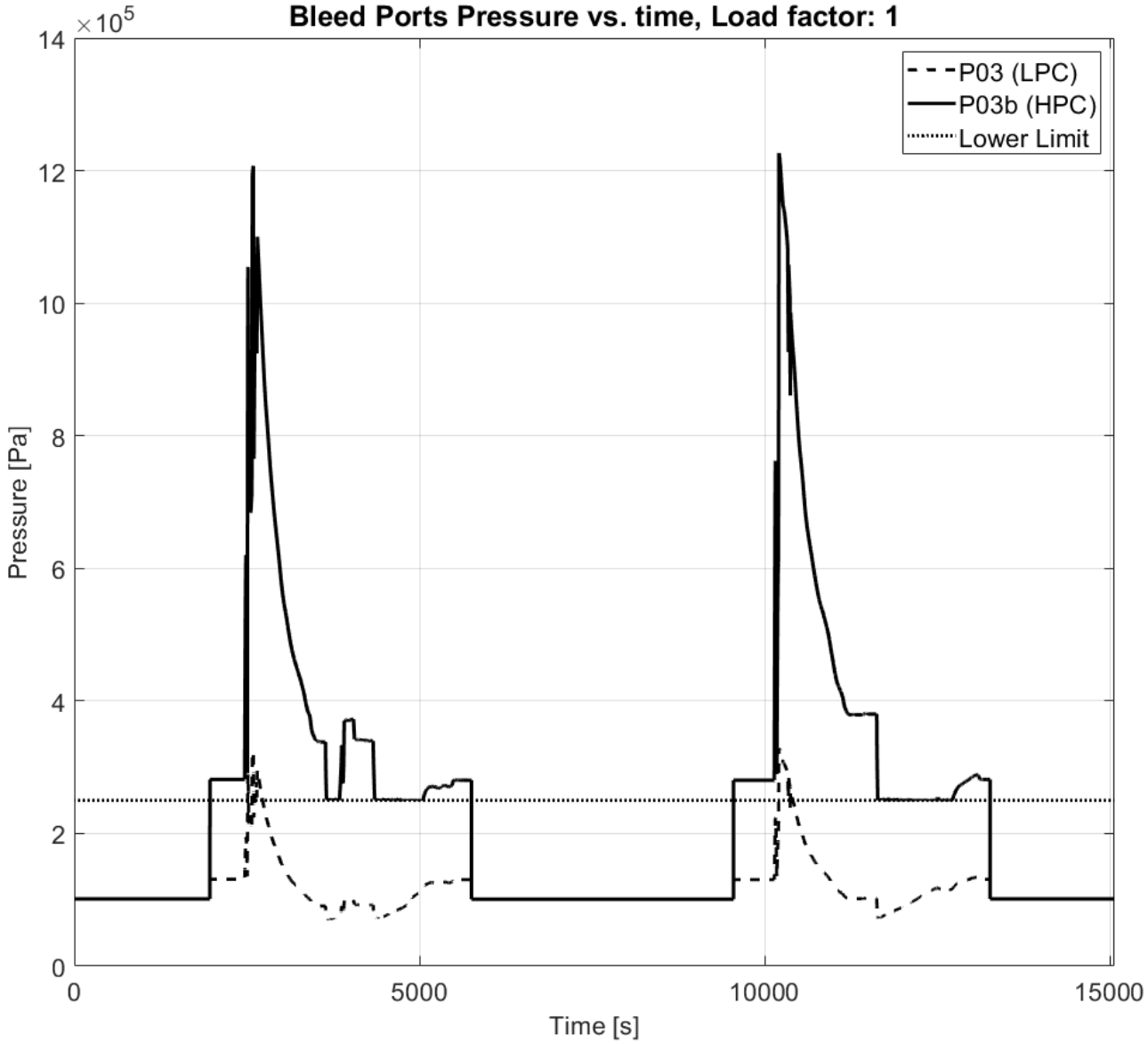

Figure 7 – Pressure at the bleed ports for the case study.

7.2.4 ECS Operational Fuel Consumption

The fuel consumption to operate the ECS can be seen in fig. 8. It is interesting to see the transition from APU to the engine's fuel consumption in the graph. The fuel consumption steps up for the ACM because bleed air temperature from the engines is higher. But for the electric machines, the fuel consumption steps down. This is explained by the higher efficiency of the engines to generate electricity.

It can also be seen where minimum fuel consumption occurs for all three systems, a short moment after takeoff and before landing. This is at an altitude where internal and external heat loads for the fuselage is in balance and minimal effort is required by the ECS to maintain the temperature in the cabin. Below this "heat balance altitude" the ambient temperature is higher and cooling is needed, while flying above this altitude heating is necessary.

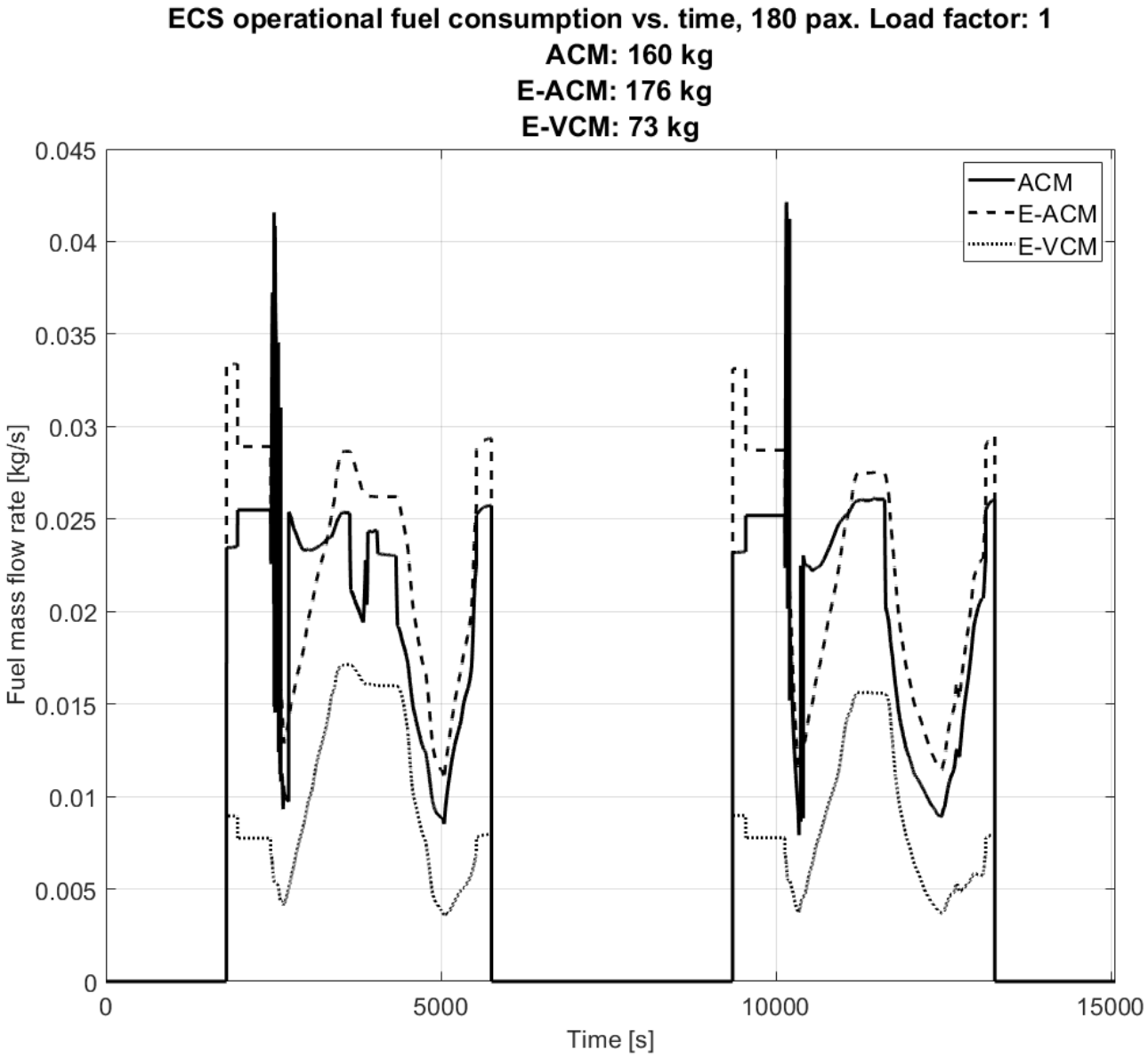

Figure 8 – ECS operational fuel consumption for the case study.

7.2.5 Effect of the Ground Temperature on the ECS Fuel Consumption

How will the temperature on the ground affect the fuel consumption for the ECS? According to the International Standard Atmosphere (ISA), the temperature at ground level is 15 °C and declining linearly down to -56.5 °C at an altitude of 11000 m. Above that altitude up to 20000 m it is constant at -56.5 °C. For the simulations, the ISA model is modified to accommodate whatever temperature there is on the ground, by simply setting the temperature on the ground and let it change linearly down to -56.5 °C at 11000 m and be constant up to 20000 m. With this simplification, it is obvious that when adjusting the ground temperature, the biggest changes will appear close to the ground.

Fig. 9 show the total ECS fuel consumption for a range of temperatures on the ground. The curves appear to be segmented and can be approximated into simple functions. Each segment represents the domination of a particular operation of the ECS. The slope of the lines correspond to the sensitivity, of each system, to the temperature change on the ground.
At lower temperature, the bleed-air driven ACM is dominated by heating operation, and it is relatively insensitive to temperature changes. The bleed-air from the engines is hot, and the ACM require little effort to heat up the cabin, even in freezing winter conditions. Above the breaking point, at around 22 °C, cooling operation dominates, and the slope is steeper. More air is flowing through the air scoops and the heat exchangers, increasing the drag and fuel consumption. The ACM and the E-ACM are essentially the same machine with the same response to the ground temperature changes. The difference between them is mostly consisting of the **ECS Forced Thrust** fuel consumption.
The E-VCM has an additional segment, revealing a feature that the other systems don't have. The fuel consumption of the E-VCM in freezing conditions dominates by the usage of the electric heater.

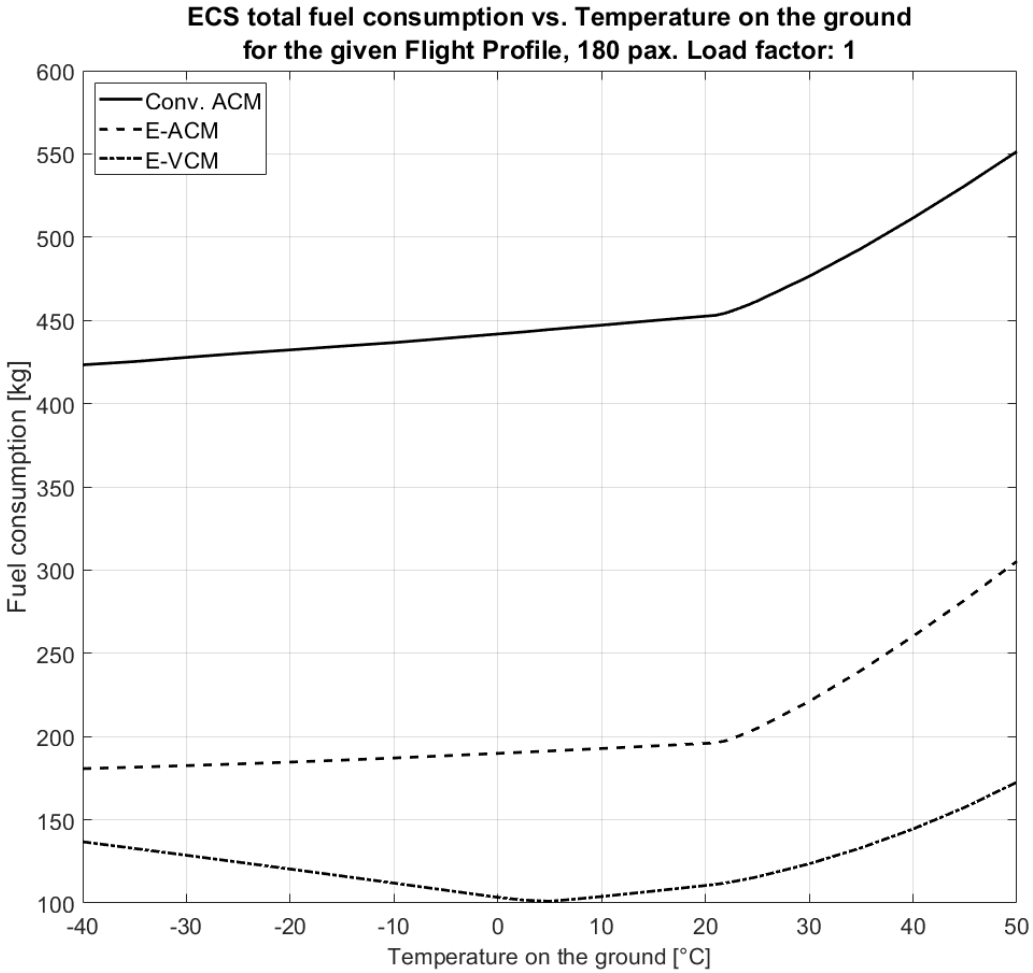

Figure 9 – ECS fuel consumption for the case study with different ground temperatures.

7.2.6 Thrust Fuel Consumption

The fuel consumption to generate thrust is plotted in fig. 10. The **ECS Forced Thrust** fuel consumption is marked as the shaded area. It is applied during the majority of the descent. The combination of low ambient pressure, at high altitude, and low thrust setting, resulted in too low bleed pressure from the engines. To maintain normal operation of the ACM, the ECS then forces the engines to run at a higher thrust setting.

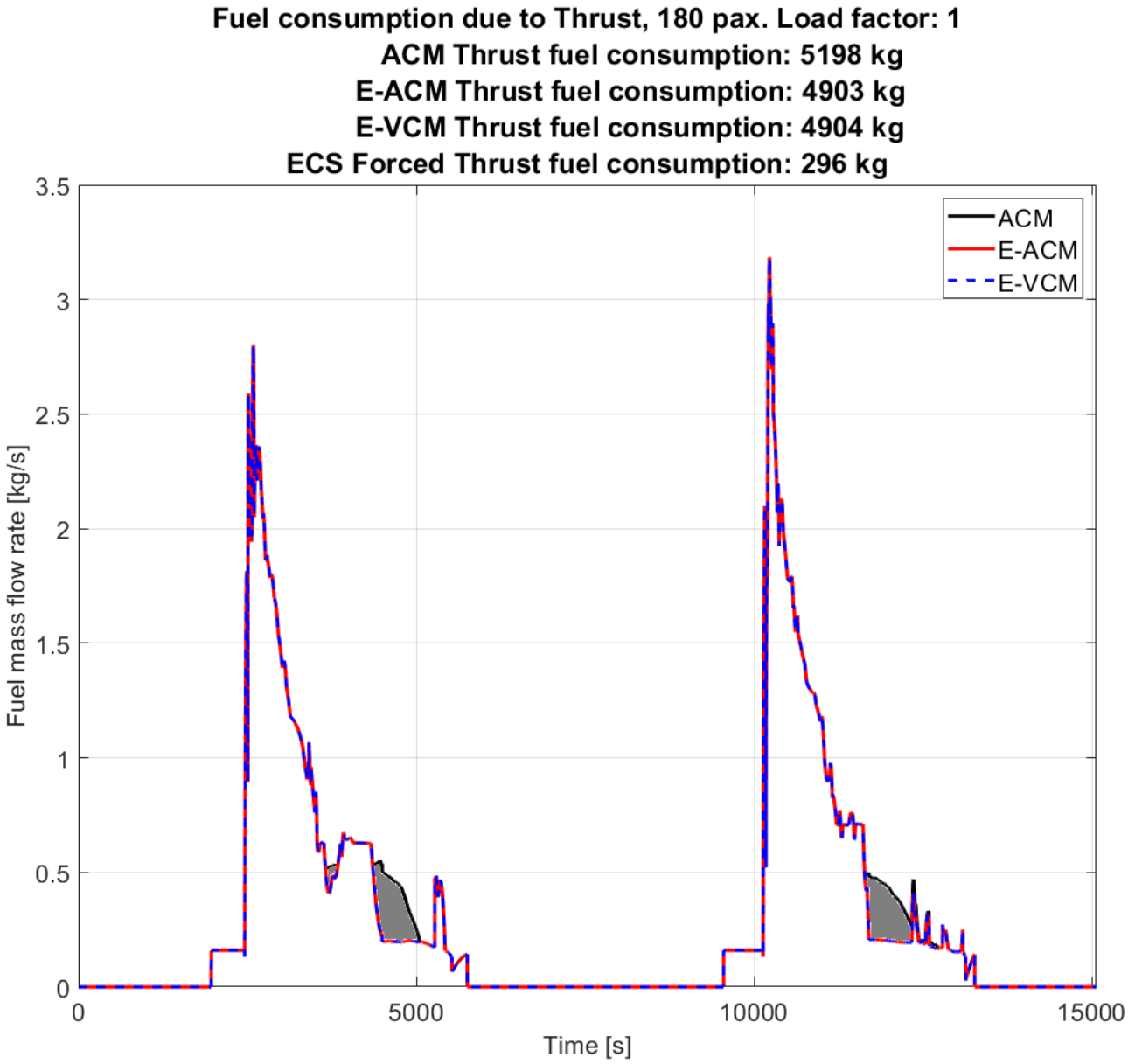

Figure 10 – Fuel consumption due to thrust and **ECS Forced Thrust** (shaded area) for the case study. E-ACM and E-VCM curves are practically identical.

7.3 Passenger Scaling Effect on Fuel Consumption

The effect of pax-scaling on the fuel consumption was investigated by running several simulations of the case study with passenger numbers from 156 to 700 pax. The result was then combined into figures to visualize the trends. First, the fuel consumption of different ECS is shown. The largest amount of fuel is used for propulsion, thus thrust fuel consumption is plotted. The fuel consumption of the whole aircraft is displayed. Lastly, the relative fuel savings are shown for all the passenger aircraft sizes in this study.

The fuel consumption of the bleed-air driven ECS can be seen in fig. 11. The coloured areas represent different aspects of the ECS that contribute to fuel consumption. The fuel consumption of the ACM **Operation**, **Weight Penalty** and **Air Scoops Drag** are almost unaffected by the pax-scaling, while the **ECS Forced Thrust** shows a noticeable relation to pax-scaling. Since thrust is firmly connected to the aircraft's weight, it can be presumed that the **ECS Forced Thrust** fuel consumption will reflect the weight per passenger of the aircraft. Compare the shape of the **ECS Forced Thrust** curve with the Aircraft Zero Fuel Mass per passenger in fig. 15.

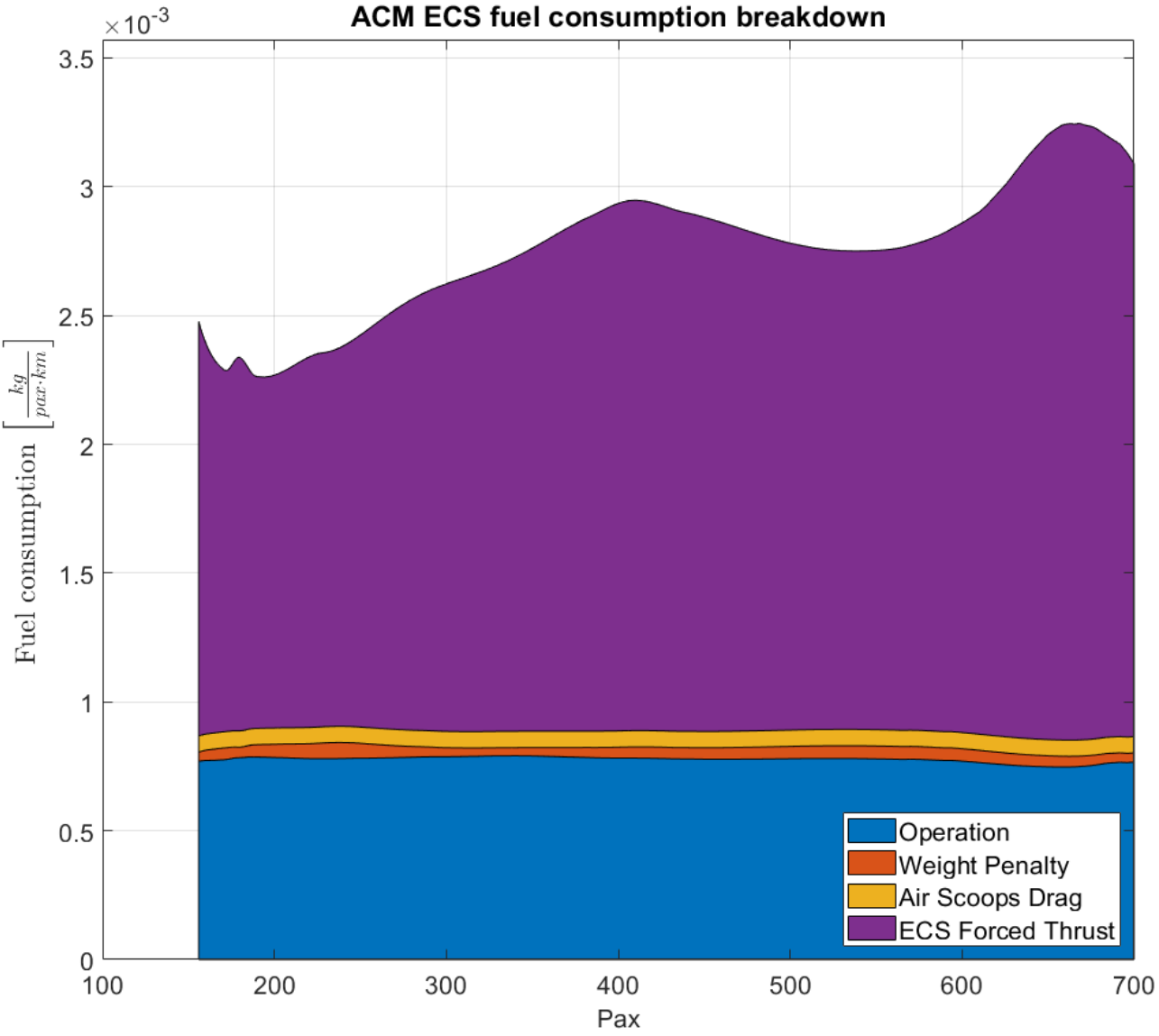

Figure 11 – Pax-scaling effect on ACM ECS fuel consumption for the case study.

Fuel consumption for the E-ACM ECS is shown in fig. 12. The greatest difference from the conventional version is that there is no **ECS Forced Thrust**. The graph shows no distinct relation to the pax-scaling.

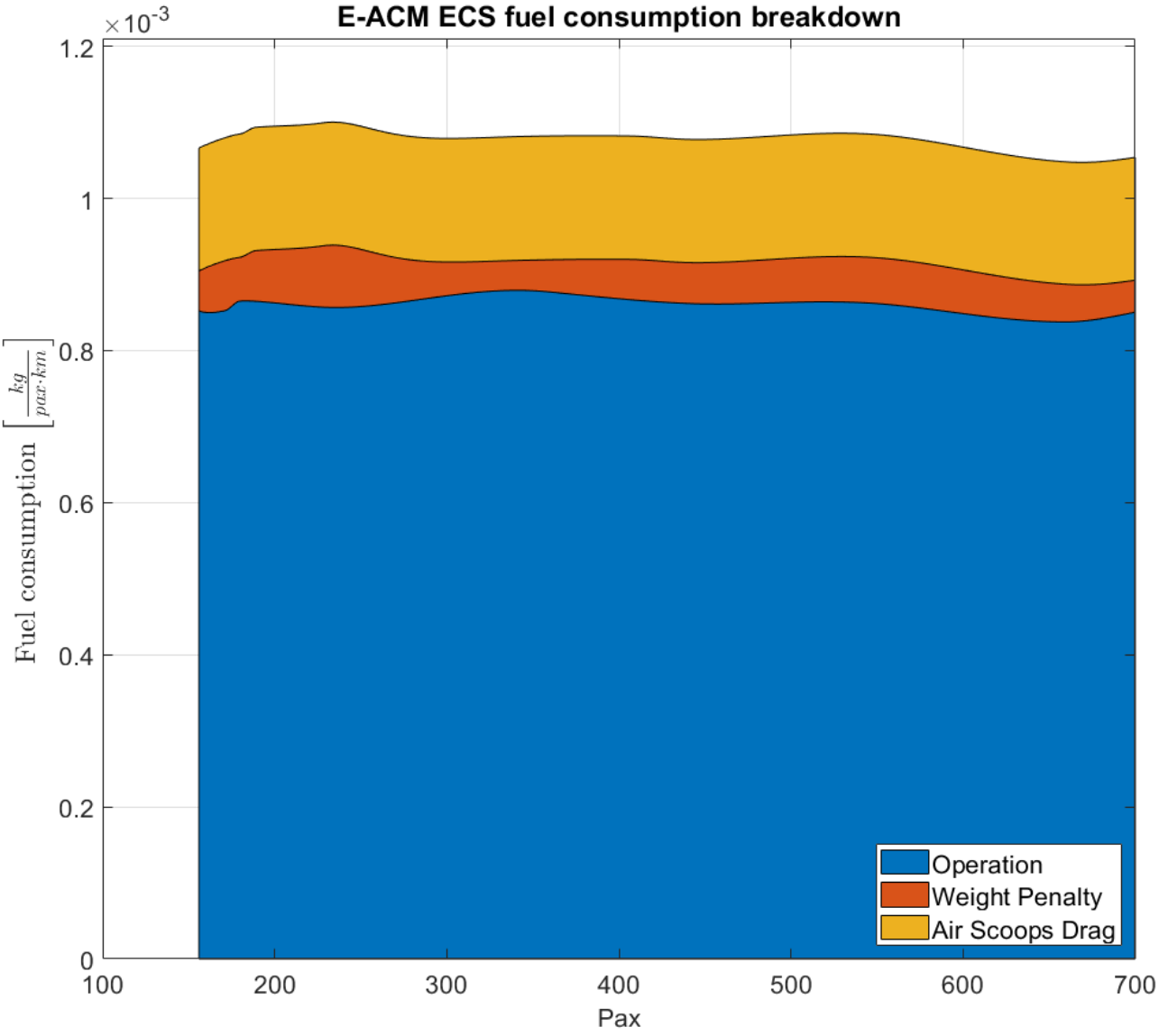

Figure 12 – Pax-scaling effect on E-ACM ECS fuel consumption for the case study.

A similar graph is shown for the E-VCM ECS. See fig. 13. The E-VCM fuel consumption does not show a clear relation to pax-scaling.

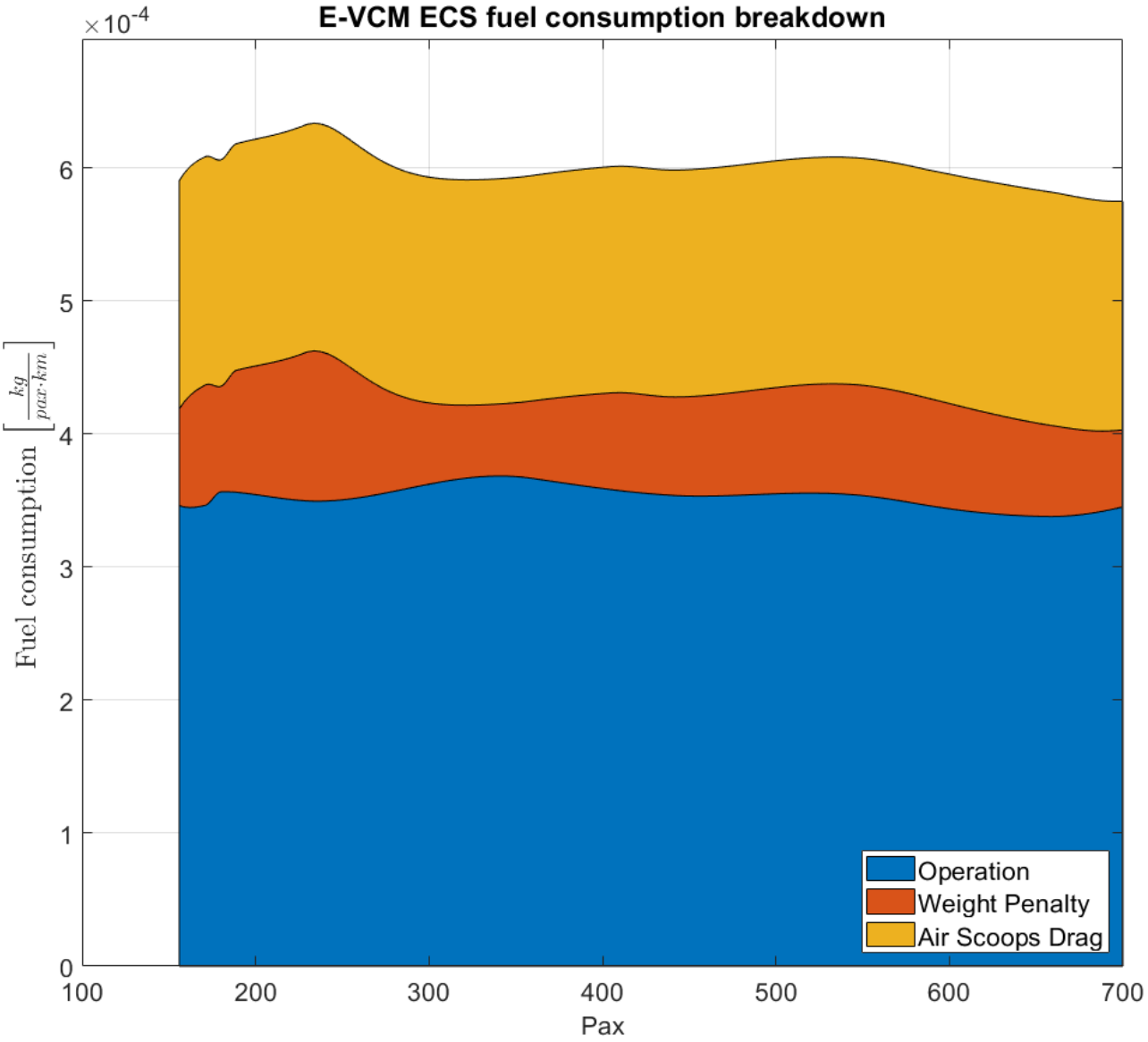

Figure 13 – Pax-scaling effect on E-VCM ECS fuel consumption for the case study.

The fuel consumption to generate thrust and its dependency on pax-scaling is plotted in fig. 14. The conventional passenger aircraft's thrust fuel consumption is higher than the MEA alternatives throughout the pax-span and is due to the **ECS Forced Thrust**. As thrust is mainly a function of weight, these curves' shapes will mostly follow the aircraft mass per passenger. Compare with fig. 15.

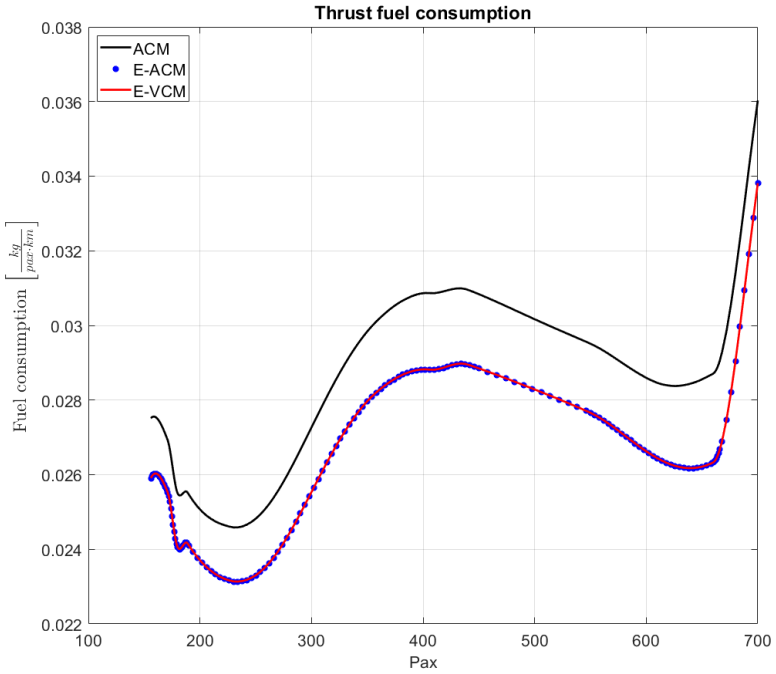

Figure 14 – Pax-scaling effect on thrust fuel consumption for the case study.

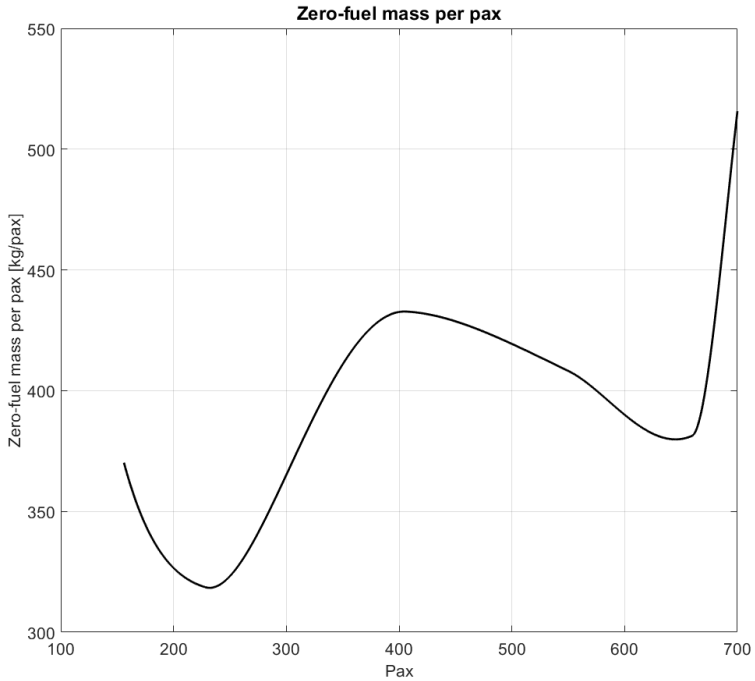

Figure 15 – Pax-scaling effect on aircraft Zero Fuel Mass per passenger.

By summing up the fuel consumption of all systems, the fuel consumption of the whole aircraft is obtained. See fig. 16.

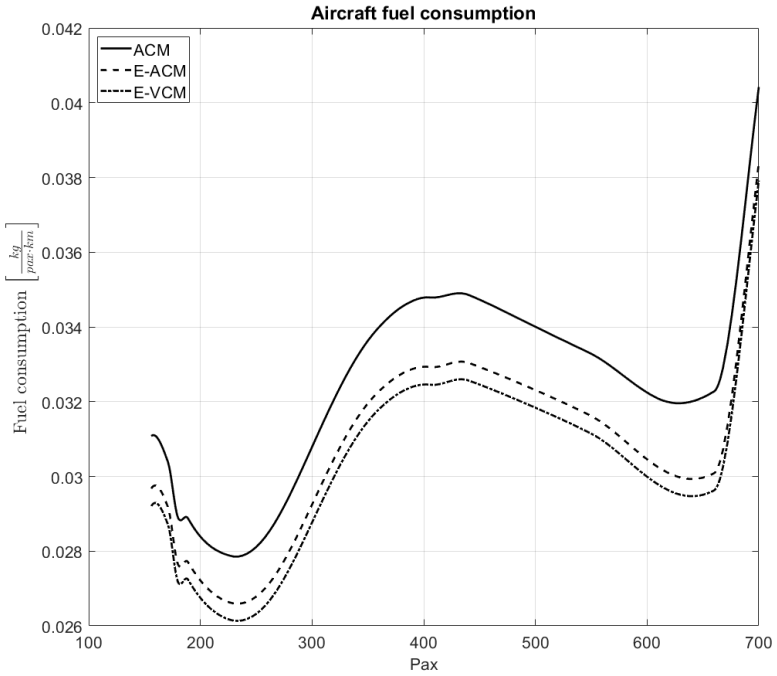

Figure 16 – Pax-scaling effect on aircraft fuel consumption for the case study.

The relative fuel savings of the aircraft with E-ACM compared to the aircraft with conventional setup can be seen in fig. 17. The graph shows an increasing trend of the relative fuel savings with the size of the passenger aircraft.

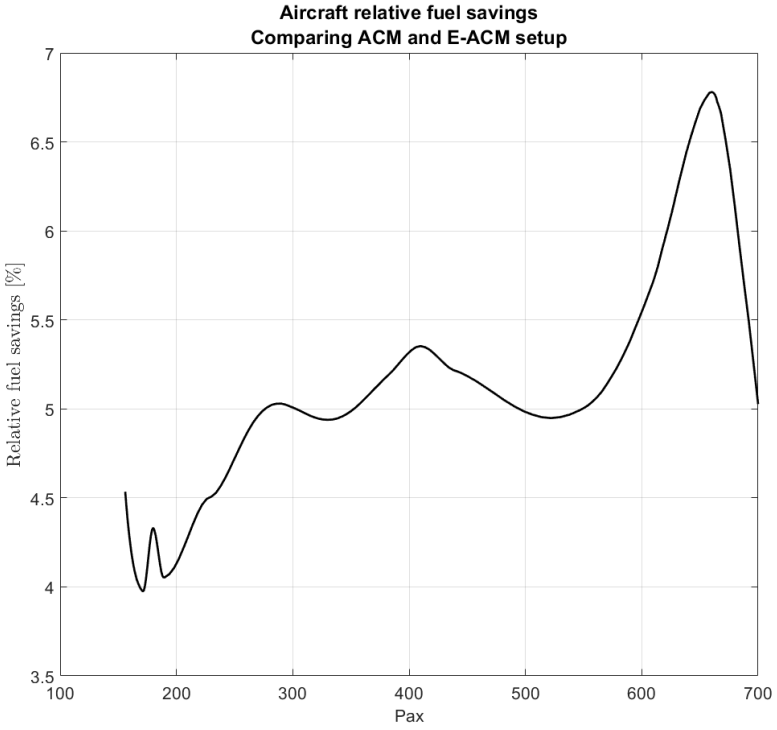

Figure 17 – Pax-scaling effect on aircraft relative fuel savings for the case study. Comparing ACM and E-ACM setup. More Electric Aircraft consumes less fuel than the conventional setup.

The relative fuel savings of the aircraft with E-VCM compared to the aircraft with conventional setup can be seen in fig. 18. The graph shows an increasing trend of the relative fuel savings with the size of the passenger aircraft.

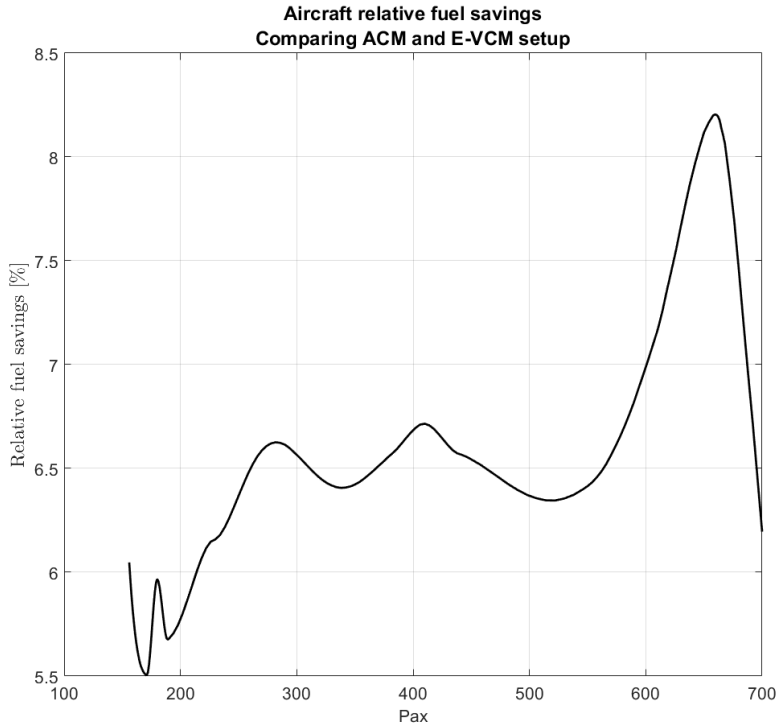

Figure 18 – Pax-scaling effect on aircraft relative fuel savings for the case study. Comparing ACM and E-VCM setup. More Electric Aircraft consumes less fuel than the conventional setup.

8. Conclusions

Calculations show that a reduction in fuel consumption is possible when electrifying the ECS. The MEA technology can therefore help the air transport industry to meet the climate goals. The main reason is the increased controllability of the compressed air without relying on the engine thrust setting. The weight penalty and increased air scoops drag of the electric ECS offset some operational fuel efficiency.

For this particular study, with passenger aircraft sizes between 156 and 700 passengers on a round trip between Copenhagen and Stockholm. The fuel savings varies between 4.0% and 6.8%, when comparing the ACM and the E-ACM setup. When comparing the ACM and the E-VCM setup, the fuel savings are even higher. It varies between 5.5% and 8.2%. The relative fuel savings increases with aircraft size.

The relative fuel savings are affected by the flight distance. The ACM setup is more efficient than the E-ACM setup during all flight phases except for the takeoff, climb and descent, where the ACM setup is penalized by high bleed-air temperature and the **ECS Forced Thrust**. For longer flight distances, when the mentioned flight phases becomes smaller parts of the flight, the differences in fuel consumption between ACM and E-ACM setup will also be less.

The numerical model can handle various passenger aircraft configurations and sizes, along with different flight profiles and conditions.

The goal was to compare many subsystems of the passenger aircraft, both conventional and electric. Due to time constrain, only three types of ECS are included in the model, thus limiting the levels of electrification. More subsystems can be added in the modular code.

Fuel consumption calculations are not easy to do, as all subsystems interact dynamically, affecting each other's power usage. The fuel consumption also depends on many conditions. There is plenty of room for improvement. The Numerical Model can be calibrated to fit a specific aircraft, or one can

introduce different Aircraft Profiles and Engine Models to make the simulations more versatile and accurate. More subsystems may be electrified and integrated. It is also recommended to try many Flight Profiles, different distances and weather conditions.

9. Contact Author Email Address

Emil Holmgren: lime@kth.se
Dhruv Haldar: haldar@kth.se
Lina Bertling Tjernberg: linab@kth.se
Andreas Johansson: andreas.x.johansson@saabgroup.com

10. Copyright Statement

References

[1] Advisory Council for Aviation Research and Innovation in Europe (ACARE). Protecting the environment and the energy supply. Url: https://www.acare4europe.org/sria/flightpath-2050-goals/protecting-environment-and-energy-supply-0 . Accessed 23 January 2022.

[2] Yildiz M. On more electric airplane: case study Stockholm - Copenhagen. Master's thesis, KTH Royal Institute of Technology, 2019.

[3] Scholz D, Seresinhe R, Staack I and Lawson C. Fuel consumption due to shaft power off-takes from the engine. *4th International Workshop on Aircraft System Technologies (AST 2013)*, Hamburg, Germany, pp. 169–179, 2013. Available online: https://www.fzt.haw-hamburg.de/pers/Scholz/Off-Takes/Off-Takes_PUB_AST-CD-Version_13-04-23.pdf

[4] Code of Federal Regulations by the Federal Aviation Administration (FAA). Code of Federal Regulations. Url: https://www.ecfr.gov/current/title-14/chapter-I/subchapter-C/part-25#25.831. Accessed 28 January 2022.

[5] Hunt E H, Reid D H, Space D R and Tilton F E. Commercial airliner environmental control system: Engineering aspects of cabin air quality. *Aerospace Medical Association annual meeting*, Anaheim, California, pp. 1–8, 1995. Available online: https://web.archive.org/web/20120331055732/http://www.cabinfiles.com/?CFrequest=file;03032001100119. Accessed 18 May 2022.

[6] Cottony H V, Dill R S. *Building materials and structures report BMS64 Solar heating of various surfaces*. United States Government Printing Office, Washington, 1941. Available online: https://nvlpubs.nist.gov/nistpubs/Legacy/BMS/nbsbuildingmaterialsstructures64.pdf

[7] Slingerland R, Zandstra S. Bleed air versus electric power off-takes from a turbofan gas turbine over the flight cycle. *7th AIAA Aviation Technology, Integration and Operations Conference (ATIO)*, Belfast, Northern Ireland, vol. 2, no. September, pp.1516–1527, 2007. Available online: https://www.researchgate.net/publication/268571644_Bleed_Air_versus_Electric_Power_Off-takes_from_a_Turbofan_Gas_Turbine_over_the_Flight_Cycle

[8] Martínez I. Aircraft environmental control. Available online: http://webserver.dmt.upm.es/~isidoro/tc3/Aircraft%20ECS.pdf

[9] Merzvinskas M, Bringhenti C, Tomita J T, De Andrade R. Air conditioning systems for aeronautical applications: A review. *Aeronautical Journal*, Vol. 124, no. 1274, pp. 499–532, 2020. Available online: https://www.cambridge.org/core/journals/aeronautical-journal/article/abs/air-conditioning-systems-for-aeronautical-applications-a-review/2ACB28C145158B38CD2437CDEBAF1350